JOURNAL OF SOLID STATE CHEMISTRY **68**, 52–60 (1987)

$(Ni_xMg_{1-x})_{10}Ge_3O_{16}$: A New Phase with Structure Related to Olivine and Spinel

J. BARBIER

Department of Geology, University of Western Ontario, London, Ontario, Canada N6A 5B7

Received May 14, 1986; in revised form August 25, 1986

A new compound, $(Ni_xMg_{1-x})_{10}Ge_3O_{16}$ ($x \simeq 0.4$–0.5), has been identified at atmospheric pressure in the NiO–MgO–GeO_2 system. Its unit cell is rhombohedral with the (hexagonal) parameters $a = 5.887(1)$ Å, $c = 28.603(4)$ Å, and $Z = 3$ for a phase with the $Ni_4Mg_6Ge_3O_{16}$ composition. A structural model has been derived from powder X-ray diffraction data: the $M_{10}Ge_3O_{16}$ (M = Ni + Mg) structure results from a regular intergrowth of {111} layers of the spinel and rock-salt structures. It can also be described as an intergrowth of (001) olivine layers (*Pnma* setting) with {111} layers of a cation-deficient rock-salt structure. Due to its close relationship to both spinel and olivine, the $M_{10}Ge_3O_{16}$ (M = Ni + Mg) structure could possibly occur at the phase boundary involved in the polymorphic olivine ⇄ spinel transformation.

Introduction

The phase relations in the NiO–MgO–GeO_2 system have been investigated at atmospheric pressure and temperatures up to 1200°C by Navrotsky (*1*) while the Ni_2GeO_4 (spinel)–Mg_2GeO_4 (olivine) join had also been previously studied at 1200°C by Reinen (*2*) and at 1400°C by Ringwood (*3*). The binary phases known in this system include Ni_2GeO_4, Mg_2GeO_4, $MgGeO_3$, and $Mg_{14}Ge_5O_{24}$, the crystal structure of which has been determined by Von Dreele *et al.* (*4*). Navrotsky (*1*) reported the absence of any ternary phase apart from the spinel and olivine solid solutions on the Ni_2GeO_4–Mg_2GeO_4 join and a limited solid solution near the $MgGeO_3$ (orthoenstatite) composition.

During the course of a reinvestigation of the Ni_2GeO_4–Mg_2GeO_4 join at elevated temperatures (1200–1600°C) and 1 atm pressure, I have, however, identified a new ternary phase, $(Ni_xMg_{1-x})_{10}Ge_3O_{16}$, with a composition range covering at least the x = 0.4–0.5 interval. This compound is shown in the NiO–Ni_2GeO_4–Mg_2GeO_4–MgO phase diagram in Fig. 1 and the determination and description of its crystal structure are the object of the present paper.

Experimental

Syntheses were carried out by high-temperature sintering of component oxides: appropriate amounts of high-purity (99.99% or better) NiO, MgO, and GeO_2 powders were mixed, pressed into pellets, and reacted at 1100°C for 3 days with intermediate remixing operations. A portion of the product was then sealed in a platinum tube, heated at 1400°C for 1 day, and finally quenched in air. The use of sealed platinum

0022-4596/87 $3.00

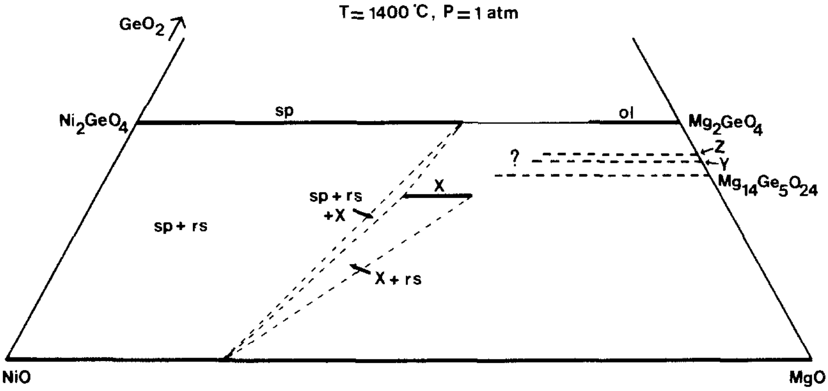

$X = (Ni,Mg)_{10}Ge_3O_{16}$
$Y = (Ni,Mg)_{18}Ge_7O_{32}$
$Z = (Ni,Mg)_{22}Ge_9O_{40}$

FIG. 1. Schematic phase diagram of the NiO–MgO–GeO_2 system at 1400°C and 1 atm pressure. The spinel and olivine solid solutions on the Ni_2GeO_4–Mg_2GeO_4 join are taken from Ringwood (*3*). The "rock-salt (rs) + X" triangle has been tentatively drawn based on data obtained by Navrotsky (*1*). The composition ranges of the phases $M_{14}Ge_5O_{24}$, $M_{18}Ge_7O_{32}$, and $M_{22}Ge_9O_{40}$ have not yet been determined.

capsules was necessary in order to prevent evaporation of GeO_2.

The nature of the reaction products was checked by powder X-ray diffraction with a Guinier–Hagg focusing camera using strictly monochromatized copper radiation ($\lambda_{K\alpha_1}$ = 1.5406 Å) and silicon as an internal standard (a = 5.4305 Å). Unit-cell parameters were refined by means of local least-squares refinement programs and X-ray diffraction line intensities were measured with a fully computerized Rigaku Geigerflex powder diffractometer.

Samples were also examined by electron diffraction using a Jeol 100CX electron microscope equipped with a double tilt (±60°) side-entry goniometer stage. For this purpose, a finely ground powder was dispersed in 1-butanol and deposited on a holey carbon film supported by a copper grid.

Characterization of $(Ni_xMg_{1-x})_{10}Ge_3O_{16}$

The new compound was first observed together with (Ni,Mg)O in the reaction products from the slow decomposition (via evaporation of GeO_2) of $(Ni_{0.4}Mg_{0.6})_2GeO_4$ spinel heated at 1400°C in air for 1 day. After 2 days at 1400°C, only (Ni,Mg)O was identified in the reaction product with a Ni/Mg ratio (determined from lattice parameter measurements) equal to that of the starting spinel phase. It may be pointed out here that the spinel phase with the composition $(Ni_{0.4}Mg_{0.6})_2GeO_4$ was found to be stable at 1400°C when heated in a sealed Pt capsule for 3 days. This result is consistent with those obtained by Ringwood (*3*) and Reinen (*2*) but not with the phase diagram determined by Navrotsky (*1*).

In order to locate the exact composition of the new compound, several samples were prepared with bulk compositions on the $(Ni_{0.4}Mg_{0.6})_2GeO_4$–$(Ni_{0.4}Mg_{0.6})O$ join. A sample with nominal composition $Ni_4Mg_6Ge_3O_{16}$, synthesized at 1250 and 1400°C, yielded a single-phase product, the X-ray powder diffraction pattern of which is given in Table I. With the help of an automatic indexing program by Visser (*5*), this diffraction pattern could be indexed on a rhombohedral unit cell with the (hexagonal) parameters a = 5.887(1) Å, c = 28.603(4) Å, and Z = 3. (The corresponding rhombohedral parameters are a = 10.122 Å, α = 33.8°, and Z = 1.) The symmetry and approximate dimensions of the $Ni_4Mg_6Ge_3O_{16}$ unit cell have also been confirmed by electron diffraction from microscopic single crystals: Figures 2a–2c show the $[01\bar{1}0]$, $[\bar{1}100]$, and $[\bar{1}010]$ zone-axis electron diffraction patterns (with hexagonal indexing) recorded from the same crystal tilted about c^*.

TABLE I

POWDER X-RAY DIFFRACTION PATTERN OF $Ni_4Mg_6Ge_3O_{16}$ INDEXED ON A RHOMBOHEDRAL UNIT CELL WITH THE FOLLOWING (HEXAGONAL) PARAMETERS: a = 5.887(1) Å, c = 28.603(4) Å, and Z = 3

$h\ k\ l$	d_{cal}	d_{obs}	I_{ca}[a]	I_{obs}[b]
0 0 3	9.534	9.494	1.7	1.3
1 0 1	5.019	5.109	7.9	10.7
0 1 2	4.802	4.803	7.2	13.8
0 0 6	4.767	4.766	9.0	
1 0 4	4.151	—	0.	—
0 1 5	3.806	3.808	27.8	27.3
1 0 7	3.1883	3.1884	4.0	11.1
0 0 9	3.1781	3.1782	3.2	2.1
1 1 0	2.9433	2.9437	16.9	23.9
0 1 8	2.9272	2.9269	19.3	25.7
1 1 3	2.8124	2.8121	29.6	25.7
0 2 1	2.5389	2.5388	24.2	27.2
2 0 2	2.5094	2.5057	6.4	82.4
1 1 6	2.5044		70.2	
1 0 10	2.4944	2.4938	34.7	47.5
0 2 4	2.4010	2.4001	18.1	22.1
0 0 12	2.3835	2.3836	5.9	2.6
2 0 5	2.3283	2.3287	35.9	33.0
0 1 11	2.3163	2.3158	7.4	10.8
0 2 7	2.1627	2.1603	3.1	4.5
1 1 9	2.1595		2.5	
2 0 8	2.0755	2.0760	100.	100.
1 0 13	2.0201	2.0200	5.5	5.0
2 1 1	1.9225	—	1.3	—
1 2 2	1.9096	—	1.0	—
0 0 15	1.9068	1.9060	3.4	3.4
0 2 10	1.9030	1.9029	2.4	
0 1 14	1.8964	—	0.	—
2 1 14	1.8605	—	0.	—
1 1 12	1.8523	—	0.	—
1 2 5	1.8260	1.8254	7.2	8.0
2 0 11	1.8203	1.8199	16.6	12.4
2 1 7	1.7428	—	1.2	—
3 0 0	1.6993	1.6989	3.4	3.5
1 2 8	1.6962	1.6956	7.2	8.4
1 0 16	1.6869	1.6874	3.3	2.9
3 0 3	1.6730	1.6726	5.9	6.4
0 2 13	1.6655	—	0.	—
3 0 6	1.6007	1.6005	16.8	26.0
1 1 15	1.6003	—	0.	
2 1 10	1.5981	1.5978	16.8	
0 1 17	1.5977	—	0.	
2 0 14	1.5942	—	1.5	—
0 0 18	1.5890	—	0.	—
1 2 11	1.5481	1.5480	4.2	4.6
3 0 9	1.4985	1.4990	0.7	1.2
2 2 0	1.4717	1.4720	64.9	72.0
0 2 16	1.4636	1.4642	63.4	66.5

[a] Intensities calculated for the structural model depicted in Fig. 3.

[b] Integrated intensities measured with a fully computerized Rigaku–Geigerflex powder diffractometer.

As indicated in the phase diagram in Fig. 1, the $(Ni,Mg)_{10}Ge_3O_{16}$ phase exists over a range of composition including the interval x = Ni/(Ni + Mg) = 0.4 to x = 0.5. In the nickel-rich region, a sample with a nominal composition $Ni_8Mg_2Ge_3O_{16}$ yielded a mixture of spinel and (Ni,Mg)O rock-salt phases, in agreement with the phase diagram published by Navrotsky (*1*). Accordingly a boundary line and a three-phase intermediate region have been drawn in Fig. 1 even though their exact locations are not known. (The point on the NiO–MgO join is taken from Navrotsky's data (*1*).) The phase diagram on the magnesium-rich side appears to be more complex due to the occurrence of several other new phases (cf.

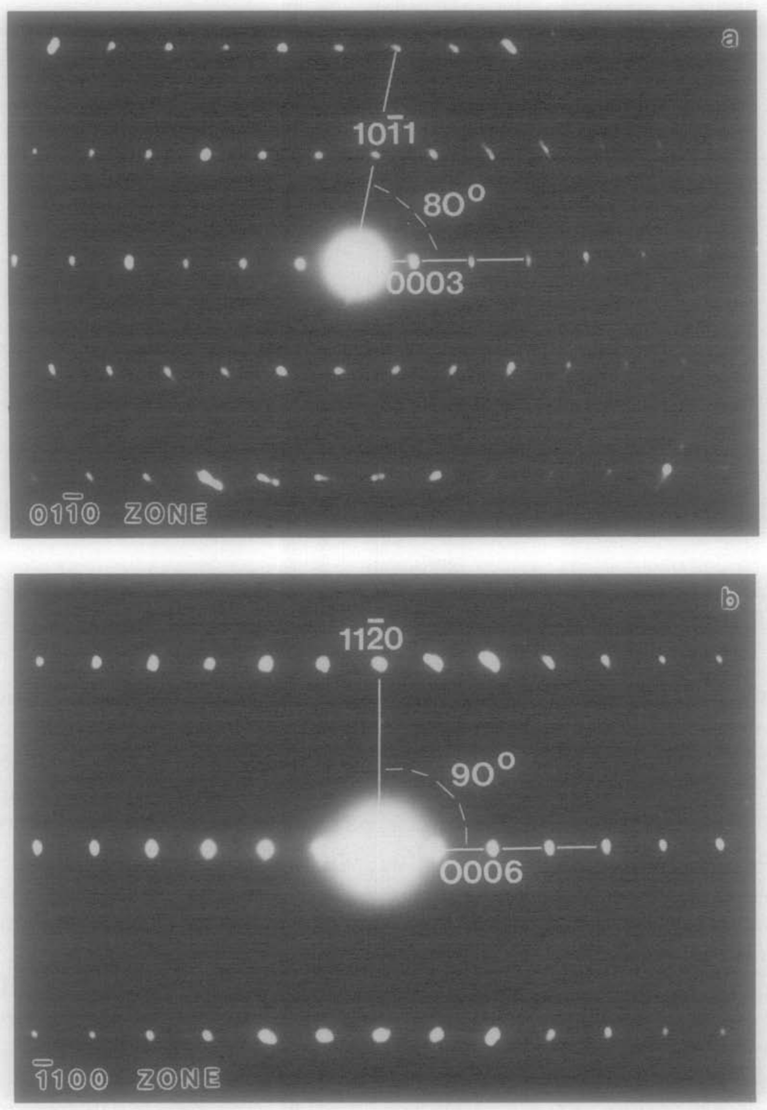

FIG. 2. (a–c) $[01\bar{1}0]$, $[\bar{1}100]$, and $[\bar{1}010]$ zone-axis electron diffraction patterns (hexagonal indexing) recorded from a single $(Ni,Mg)_{10}Ge_3O_{16}$ microcrystal tilted around c^*_{hex}. The observed interplanar angles are equal to the angles calculated for the rhombohedral unit cell given in Table I.

below) and no experimental data have been obtained for this region.

The $(Ni,Mg)_{10}Ge_3O_{16}$ phase was observed to be stable at least up to 1400°C at atmospheric pressure. However, when heated at 1600°C for 1 hr in a sealed Pt capsule, it decomposed completely into (mainly) a mixture of (Ni,Mg)O rock-salt plus a new phase later identified as $(Ni,Mg)_{22}Ge_9O_{40}$. The decomposition reaction can then be formulated as follows:

$$3\ (Ni,Mg)_{10}Ge_3O_{16} \rightarrow (Ni,Mg)_{22}Ge_9O_{40} + 8\ (Ni,Mg)O.$$

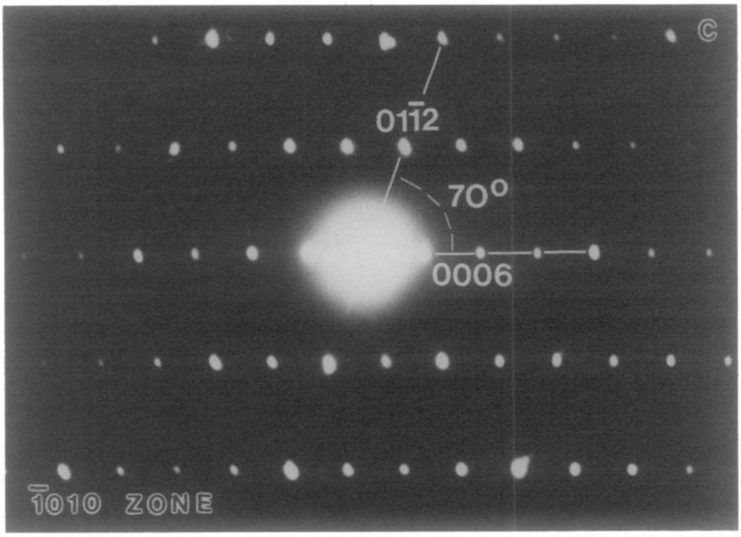

FIG. 2—*Continued.*

In fact, examination of the reaction product by high-resolution electron microscopy revealed the presence of minor amounts of two other phases resulting from similar reactions and identified as $(Ni,Mg)_{14}Ge_5O_{24}$ and $(Ni,Mg)_{18}Ge_7O_{32}$. Together with $(Ni,Mg)_{10}Ge_3O_{16}$ and $(Ni,Mg)_{22}Ge_9O_{40}$, these phases have been shown to form a new structural family represented by the general formula $M_{4n+6}Ge_{2n+1}O_{8(n+1)}$ (M = Ni + Mg; $n = 1, 2, 3, 4$) in which the member $n = 1$ corresponds to the $M_{10}Ge_3O_{16}$ structure described here, the member $n = 2$ is isostructural with $Mg_{14}Ge_5O_{24}$ (*4*), and the $n = \infty$ end-member is olivine. A characterization of this new homologous series by high-resolution electron microscopy will appear elsewhere (*6*).

Description of the $(Ni,Mg)_{10}Ge_3O_{16}$ Structure

The cell parameters determined for $Ni_4Mg_6Ge_3O_{16}$ (cf. above) suggested that its crystal structure is based on a cubic close-packing of oxygen atoms: the ratio c/a = 4.859 is close to the ideal ratio $c/a = 6\sqrt{2}/\sqrt{3} = 4.899$ for a 12-layer cubic "close-packed" structure with $a = 5.887$ Å $= 2\,d$(O . . . O); and the rhombohedral angle $\alpha = 33.8°$ is also nearly equal to the equivalent angle $([\bar{1}1\bar{2}], [\bar{1}2\bar{1}]) = 33.6°$ in the cubic spinel structure. The composition of the new compound and its formation by decomposition of $(Ni,Mg)_2GeO_4$ spinel at high temperature (via loss of GeO_2) also suggested that its crystal structure might be simply related to that of spinel. A model was then developed which is depicted in Fig. 3, showing the ideal $(Ni,Mg)_{10}Ge_3O_{16}$ structure based on a perfect cubic "close-packed" oxygen array with metal atoms in octahedral and tetrahedral coordination.

The validity of this structural model has been checked via calculations of the intensities of the powder X-ray diffraction lines of $Ni_4Mg_6Ge_3O_{16}$. The computations were carried out by means of the program "Lazy-Pulverix" (*7*), all atoms being placed in the special positions 1(*a*) and 3(*b*) of the $R3m$ space group with the following atomic coordinates and cation distribution:

Ge(1)	1(*a*)	0, 0, 0,	
Ge(2)	1(*a*)	$\frac{3}{16}, \frac{3}{16}, \frac{3}{16}$	
Ge(3)	1(*a*)	$\frac{13}{16}, \frac{13}{16}, \frac{13}{16}$	
$M(1)$	1(*a*)	$\frac{1}{2}, \frac{1}{2}, \frac{1}{2}$	
$M(2)$	3(*b*)	$0, \frac{1}{2}, \frac{1}{2}$	$M = 0.4$ Ni $+ 0.6$ Mg
$M(3)$	3(*b*)	$\frac{3}{4}, \frac{1}{4}, \frac{1}{4}$	
$M(4)$	3(*b*)	$\frac{1}{4}, \frac{3}{4}, \frac{3}{4}$	
O(1)	1(*a*)	$\frac{1}{8}, \frac{1}{8}, \frac{1}{8}$	
O(2)	1(*a*)	$\frac{3}{8}, \frac{3}{8}, \frac{3}{8}$	
O(3)	1(*a*)	$\frac{5}{8}, \frac{5}{8}, \frac{5}{8}$	
O(4)	1(*a*)	$\frac{7}{8}, \frac{7}{8}, \frac{7}{8}$	
O(5)	3(*b*)	$\frac{5}{8}, \frac{1}{8}, \frac{1}{8}$	
O(6)	3(*b*)	$\frac{3}{8}, \frac{7}{8}, \frac{7}{8}$	
O(7)	3(*b*)	$\frac{1}{8}, \frac{5}{8}, \frac{5}{8}$	
O(8)	3(*b*)	$\frac{7}{8}, \frac{3}{8}, \frac{3}{8}$.	

This set of atomic positions led to a good agreement between calculated and observed intensities (cf. Table I) with a reliability factor $R = \Sigma|I_o - I_c|/\Sigma I_o = 15\%$, thus supporting the proposed structural model for $(Ni,Mg)_{10}Ge_3O_{16}$. This model corresponds to a random distribution of Ni and Mg atoms and the possibility of Ni/Mg ordering has not been investigated.

Comparison of the $(11\bar{2}0)_{hex}$ projection of the $(Ni,Mg)_{10}Ge_3O_{16}$ structure (Fig. 3) with the equivalent $(110)_c$ projection of the spinel structure (Fig. 4) shows a great similarity between the two: the slabs denoted "S" in $(Ni,Mg)_{10}Ge_3O_{16}$ (forming 75% of the structure) correspond to three {111} layers of the spinel structure; they alternate in the c_{hex} direction with single-layer slabs "R" with the rock-salt structure. It follows therefore that the $(Ni,Mg)_2GeO_4$ spinel → $(Ni,Mg)_{10}Ge_3O_{16}$ transformation simply involves the replacement, within the "R" layers, of $(2\ {}^{IV}Ge^{4+} + {}^{VI}M^{2+})$ by $(Ge^{4+} + 3\ {}^{VI}M^{2+})$ (where the IV and VI roman superscripts represent tetrahedral and octahedral coordination, respectively). The replacement of one tetravalent Ge atom by two divalent M =(Ni + Mg) atoms accounts for the change of stoichiometry accompanying the transformation.

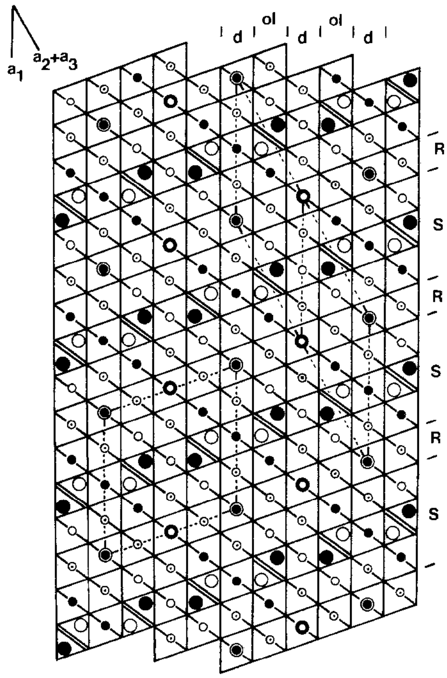

FIG. 3. The ideal $(Ni,Mg)_{10}Ge_3O_{16}$ structure projected on $(11\bar{2}0)_{hex}$. Large and small circles are Ge and (Ni,Mg) atoms, respectively. (Oxygen atoms have been omitted.) Filled, open, and dotted circles are at heights 50, 0, and ±25, respectively (expressed in units of $\frac{1}{100}$ of the repeat along the projection axis). The true primitive rhombohedral cell has been outlined as well as a one-face-centered monoclinic cell (containing two formula units) useful for comparison with other structures of the homologous series (*5*). The $(Ni,Mg)_{10}Ge_3O_{16}$ structure consists of an intergrowth of three-{111}-layer thick spinel slabs (S) and single {111} rock-salt layers (R) in the c_{hex} direction. It can alternatively be described in terms of olivine layers (ol) alternating with cation-deficient rock-salt layers (d) parallel to the $(011)_{rh}$ plane.

Since both Ni_2GeO_4 and Mg_2GeO_4 spinels have a normal cation distribution, i.e., ${}^{VI}M_2{}^{IV}GeO_4$ (*8*), the spinel slabs "S" of the $(Ni,Mg)_{10}Ge_3O_{16}$ structure are also expected to be normal, with four-coordinated Ge atoms and six-coordinated Ni and Mg atoms. The simultaneous presence of ${}^{IV}Ge$ and ${}^{VI}Ge$ atoms makes $(Ni,Mg)_{10}Ge_3O_{16}$ a rather unusual germanate compound: another such example exists with the related

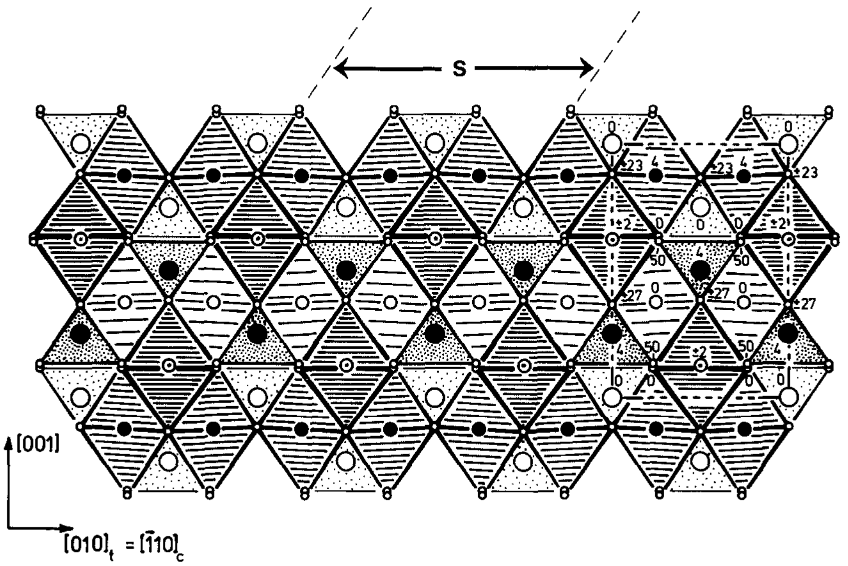

FIG. 4. The spinel structure of γ-Fe_2SiO_4 (*16*) projected on $(100)_t = (110)_c$. (The subscripts c and t refer to the conventional face-centered cubic unit cell and to the smaller body-centered tetragonal cell related to *c* by the matrix $\frac{1}{2}\frac{1}{2}0/-\frac{1}{2}\frac{1}{2}0/001$). Large, medium, and small circles are Si, Fe, and O atoms, respectively. Heights of metal and oxygen atoms are expressed in $\frac{1}{8}$ and $\frac{1}{100}$ of the a_t repeat, respectively. One "S" slab identical to those in Fig. 3 has been indicated.

phase $Mg_{14}Ge_5O_{24}$ (*4*) (cf. also below and Fig. 5).

Although its relationship to spinel provides the most obvious description of the $(Ni,Mg)_{10}Ge_3O_{16}$ structure, it is also simply related to olivine: in Fig. 3, single olivine-type layers are readily recognized, parallel to the $(011)_{rh}$ plane. (Denoted "ol," they have the stoichiometry $M_4Ge_2O_8$ and correspond to (001) layers when the unit-cell setting of olivine is *Pnma*.) In a direction perpendicular to a_1, these olivine layers alternate with single layers, "*d*," of a slightly cation-deficient rock-salt structure with stoichiometry M_6GeO_8. Accordingly the formation of $(Ni,Mg)_{10}Ge_3O_{16}$ can be formally written as

$$M_{10}Ge_3O_{16} = M_4Ge_2O_8(\text{ol}) + M_6GeO_8(\text{d}) \quad (M = \text{Ni} + \text{Mg}),$$

which suggests the possibility of varying the proportions of the two component structure types. This is indeed observed in the $Mg_{14}Ge_5O_{24}$ structure (*4*) in which (Fig. 5) double olivine layers alternate with the same single cation-deficient rock-salt layer, i.e.:

$$Mg_{14}Ge_5O_{24} = 2\ Mg_4Ge_2O_8(\text{ol}) + Mg_6GeO_8(\text{d}).$$

Other phases containing triple and quadruple olivine layers have also been identified in the NiO–MgO–GeO_2 system (*6*) forming a new structural family based on intergrowth of the olivine and cation-deficient rock-salt structure types:

$$M_{4n+6}Ge_{2n+1}O_{8(n+1)} = nM_4Ge_2O_8(\text{ol}) + M_6GeO_8(\text{d}),$$

with M = Ni + Mg and n = 1, 2, 3, and 4.

As shown in Fig. 5, the oxygen array in the $Mg_{14}Ge_5O_{24}$ structure displays some deviation from ideal "close-packing." Although some degree of distortion can also

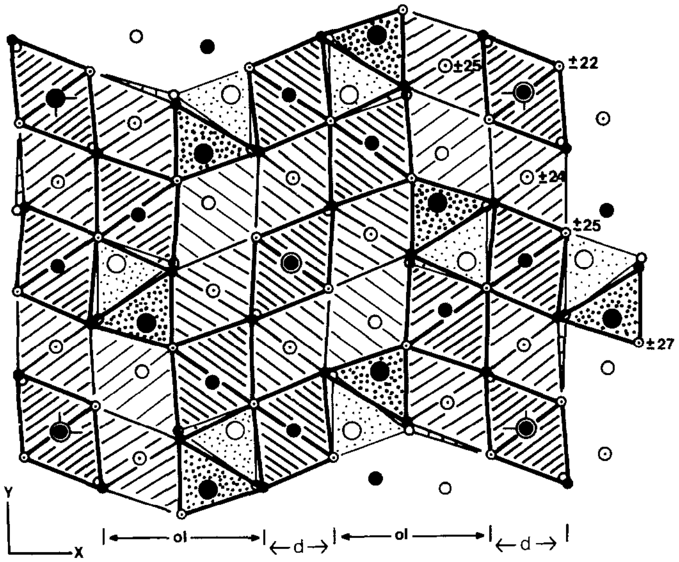

FIG. 5. The structure of Mg$_{14}$Ge$_5$O$_{24}$ (*4*) projected on (001). Large, medium, and small circles are Ge, Mg, and O atoms, respectively. Filled, open, and dotted circles are at heights 50, 0, and ≈ ±25, respectively (in units of *c*/100). Double olivine layers (ol) alternate with single cation-deficient rock-salt layers (d) in the *x* direction.

be expected in the real (Ni,Mg)$_{10}$Ge$_3$O$_{16}$ structure, it is likely to be small as estimated from the close-to-ideal cell parameters ratios (with a deviation of less than 1%; cf. above) and also from the nearly ideal spinel structures of both Ni$_2$GeO$_4$ and Mg$_2$ GeO$_4$ (with u parameters equal to 0.25 and 0.2508, respectively (*8*)).

The decomposition of (Ni,Mg)$_{10}$Ge$_3$O$_{16}$ structure at high temperature can be directly associated with the high proportion of spinellike elements in its crystal structure: just as (Ni,Mg)$_2$GeO$_4$ spinel becomes unstable with respect to olivine above a certain temperature at atmospheric pressure (the spinel → olivine transition taking place at 810°C in Mg$_2$GeO$_4$ (*9*) and above 1400°C in (Ni$_{0.4}$Mg$_{0.6}$)$_2$GeO$_4$ (*3*)), (Ni,Mg)$_{10}$Ge$_3$O$_{16}$ transforms into a series of olivine-related phases at temperatures around 1500–1600°C. Accordingly, arguments previously put forward for explaining the relative stability of the spinel and olivine structure types (e.g., *10, 11*) may also be applicable in this case. The dissociation temperature of (Ni,Mg)$_{10}$Ge$_3$O$_{16}$ can be expected to decrease with decreasing Ni/Mg ratio (by analogy with the spinel → olivine transition) leading to the speculation that, if it exists at all, a compound Mg$_{10}$Ge$_3$O$_{16}$ would only be stable at low temperature, dissociating into Mg$_{14}$Ge$_5$O$_{24}$ + MgO at higher temperature. (Mg$_{14}$Ge$_5$O$_{24}$ itself decomposes into Mg$_2$GeO$_4$ olivine + MgO at 1495°C (*12*).)

Since the (Ni,Mg)$_{10}$Ge$_3$O$_{16}$ structure contains elements of both the spinel and olivine structure types (cf. Fig. 3), it could easily form intergrowths with them and could therefore be regarded as a plausible structural intermediate in the spinel $\rightleftarrows$ olivine transformation. Such a structure could exist, for instance, at the phase boundary formed when spinel crystals are grown from olivine crystals under high-pressure, high-temperature conditions. In such a case, as is obvious from Figs. 3 and 4, the spinel/olivine orientation relationship would be given as $(001)_{ol}//(\bar{1}11)_{sp}$ and $[010]_{ol}//[110]_{sp}$ (for the *Pnma* setting of the olivine unit cell) which, indeed, corresponds to the experimental observations (e.g., growth of Ni_2SiO_4 spinel crystals by Hamaya and Akimoto (*13*)).

Just as the spinelloid structural family has been proposed as possible intermediates in a martensitic-type olivine ⇄ spinel transition (*14, 15*), one could imagine the $(Ni,Mg)_{10}Ge_3O_{16}$ structure together with other olivine-related phases of the $M_{4n+6}Ge_{2n+1}O_{8(n+1)}$ family as providing an alternative path for the same transformation. Such a mechanism would then correspond to a nucleation and growth kind of transition still consistent, however, with the experimental olivine/spinel orientation relationship.

Conclusion

The new $(Ni,Mg)_{10}Ge_3O_{16}$ structure can be regarded as intermediate between the well-known spinel and olivine structure types. The description of its crystal structure suggests that intergrowth with either olivine or spinel could be readily achieved which is indeed experimentally confirmed, in the case of olivine, by the formation of a new structural family (*6*). (Preliminary single-crystal growth experiments also indicate that macroscopic spinel/$(Ni,Mg)_{10}Ge_3O_{16}$ intergrowths are common, the phase boundary being parallel to $\{111\}_{sp}$.)

Finally, it may be pointed out that, in the course of her investigation of the CoO–MgO–GeO_2 system at 1 atm pressure, Navrotsky (*1*) reported the existence of an unidentified phase corresponding to a molar fraction $X_{GeO_2} \simeq 0.24$. It appears likely that this phase is, in fact, isostructural with $(Ni,Mg)_{10}Ge_3O_{16}$ (for which $X_{GeO_2} = 0.23$) thereby establishing an even closer similarity between the CoO– and NiO–MgO–GeO_2 systems.

Acknowledgments

Part of this work was carried out at the Research School of Chemistry, Australian National University, and financial support from ANU is acknowledged. The author is grateful to Prof. B. G. Hyde and Dr. M. E. Fleet for a critical review of the manuscript.

References

1. A. NAVROTSKY, *J. Solid State Chem.* **6,** 21 (1972).
2. D. REINEN, *Z. Anorg. Allg. Chem.* **356,** 172 (1968).
3. A. E. RINGWOOD, *Aust. J. Sci.* **378** (1961).
4. R. B. VON DREELE, P. W. BLESS, E. KOSTINER, AND R. E. HUGHES, *J. Solid State Chem.* **2,** 612 (1970).
5. J. W. VISSER, *J. Appl. Crystallogr.* **2,** 89 (1969).
6. J. BARBIER, submitted.
7. K. YVON, W. JEITSCHKO, AND E. PARTHÉ, *J. Appl. Crystallogr.* **10,** 73 (1977).
8. R. J. HILL, J. R. CRAIG, AND G. V. GIBBS, *Phys. Chem. Minerals* **4,** 317 (1979).
9. F. DACHILLE AND R. ROY, *Amer. J. Sci.* **258,** 225 (1960).
10. B. KAMB, *Amer. Mineral.* **53,** 1439 (1968).
11. M. O'KEEFFE AND B. G. HYDE, *Nature (London)* **293,** 727 (1981).
12. C. R. ROBBINS AND E. M. LEVIN, *Amer. J. Sci.* **257,** 63 (1959).
13. N. HAMAYA AND S. AKIMOTO, *Phys. Earth Planet. Inter.* **29,** 6 (1982).
14. B. G. HYDE, T. J. WHITE, M. O'KEEFFE, AND A. W. S. JOHNSON, *Z. Kristallogr.* **160,** 53 (1982).
15. M. MADON AND J. P. POIRIER, *Phys. Earth Planet. Inter.* **33,** 31 (1983).
16. F. MARUMO, M. ISOBE, AND S. AKIMOTO, *Acta Crystallogr. B* **33,** 713 (1977).